ISSUE: November 2023

How Active EMI Filter ICs Reduce Common-Mode Emissions In Single- And Three-Phase Applications (Part 1): An Overview

by Timothy Hegarty, Texas Instruments, Phoenix, Ariz.

Automotive onboard chargers (OBCs) and aerospace power supplies are examples of highly constrained system environments where volumetric and gravimetric power densities are important metrics. It's important to reduce the volume of the electromagnetic interference (EMI) input filter components so that the solution can fit into demanding form factors. As a result, a compact and efficient design of the EMI input filter is one of the main challenges in a high-density switching regulator, and is vital to achieving the full benefits of electrification in automotive, enterprise, aerospace and other highly constrained system environments.

Common-mode (CM) filters for both commercial (Class A) and residential (Class B) environments typically have limited Y-capacitance because of touch-current safety requirements,[1,2] and thus require large-sized CM chokes to achieve the requisite attenuation. This ultimately results in filter designs with bulky, heavy and expensive passive components. Using active EMI filter (AEF) circuits enables more-compact filter solutions for next-generation power-conversion systems.[3]

It is possible to further optimize space-constrained applications such as those mentioned above by leveraging active filter integrated circuits (ICs) to significantly reduce magnetic components and overall filter size. Further benefits include lower power losses for better thermal management, easier system-level packaging designs, reduced electromagnetic coupling among components within a confined space, and lower costs.

This article introduces the topic of active EMI filtering and provides practical circuit realizations using a new family of standalone AEF ICs for CM noise mitigation in single- and three-phase systems. Measured results from a 3.3-kW totem-pole PFC stage will illustrate the benefits of EMI reduction and board space savings.

This article begins with a review of conducted EMI standards across the frequency spectrum, discussing how new requirements at lower frequencies will tend to increase space requirements for conventional, passive EMI filters. Popular configurations of passive EMI filters for kilowatt-level, grid-connected applications are then presented with discussion of how safety requirements constrain component selection, leading to bulkier designs.

With that as background, the principles underlying operation of active EMI filters and the related hybrid EMI filters are explained. This is followed by more details on the CM active filter circuit based on the voltage-sense current-inject (VSCI) method and its advantages. In addition, this circuit's mechanism for Y-capacitor multiplication is explained.

Schematics of practical AEF circuits based on TI's single-phase TPSF12C1 and three-phase TPSF12C3 AEF ICs are then presented. Finally, experimental results (CM noise measurements) are given for an implementation based on a TPSF12C1 evaluation module, and its benefits with respect to choke size and other parameters are discussed along with some design tradeoffs.

EMI Standards And Frequency Ranges

High-frequency switching networks, while being essential components for energy conversion in switched-mode ac-dc regulators, are also inherent sources of input current harmonics and conducted EMI that can affect the normal operation of adjacent equipment sharing the same grid-connected input source. Fig. 1 depicts the harmonic and conducted EMI frequency ranges classified by electromagnetic compatibility (EMC) standards organizations such as IEC and CISPR.

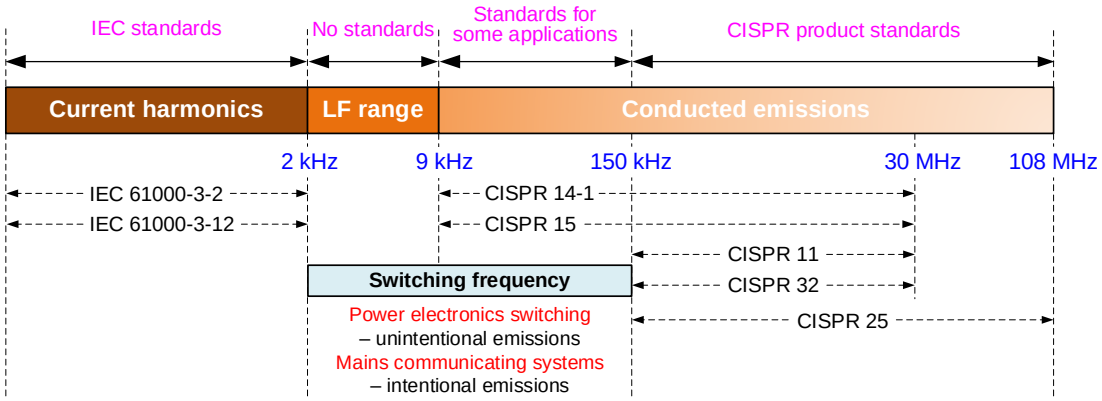

Fig. 1. Harmonic current and conducted EMI frequency ranges classified by the IEC and CISPR.

Applying PFC techniques enables the input current harmonics to meet limits set by IEC 61000-3-2 and IEC 61000-3-12 at frequencies up to 2 kHz. EMI filters are still mandatory, however, in order to attenuate high-frequency noise currents and meet conducted emissions specifications (such as CISPR 11 for industrial and CISPR 25 for automotive applications) within classified frequency ranges beginning at 150 kHz,[4] as illustrated in Fig. 2.

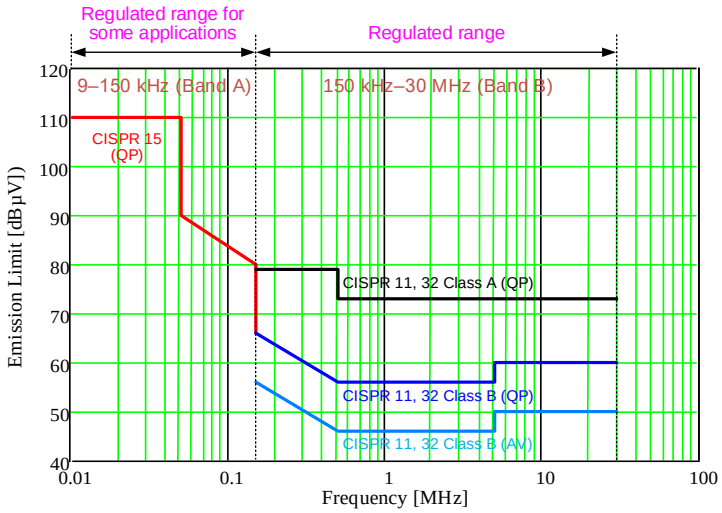

Fig. 2. CISPR limits using quasi-peak and average detectors in the frequency range of 9 kHz to 30 MHz.

Moreover, given the penetration of medium- and high-power systems with switching frequencies lower than 100 kHz, multiple working groups in IEC SC77A are presently focused on extending emissions limits below 150 kHz. This distinguishes an emerging conducted EMI frequency range of 2 kHz to 150 kHz, which the IEC splits into two main bands, 2 kHz to 9 kHz and 9 kHz to 150 kHz. The latter is classified as the Class A band in CISPR 16 and has received particular scrutiny, as powerline communications systems also use this band for smart-grid applications.

IEC 61000-2-2 already defines compatibility levels for mains communicating systems in the 9- to 150-kHz frequency range, which may later be used by standards bodies as a template to set emission limits at the product level. With standardization activities ongoing, the forthcoming addition of the 9- to 150-kHz band and applicable emissions limits to the existing IEC 61000-6-3 generic EMI standard[4] may affect the future design of EMI filters for attenuation below 150 kHz.

EMI mitigation across wide frequency ranges will require correspondingly larger passive components. As Fig. 1 and Fig. 2 indicate, only the CISPR 14-1 and CISPR 15 product standards—for household appliances and lighting applications, respectively—presently specify emissions limits as low as 9 kHz. It is clear that upcoming filter designs with mitigation at lower frequencies will require correspondingly larger passive components.

Passive EMI Filters For Grid-Powered Applications

Complying with EMC regulations intended to limit the levels of conducted emissions requires the insertion of a low-pass EMI filter between a switching regulator and its mains input source. Fig. 3 illustrates typical filter arrangements for single-phase, three-phase (three-wire, no neutral) and three-phase (four-wire with neutral) systems in kilowatt-scale, grid-connected applications. L, N and PE refer to live, neutral and protective earth terminals, respectively.

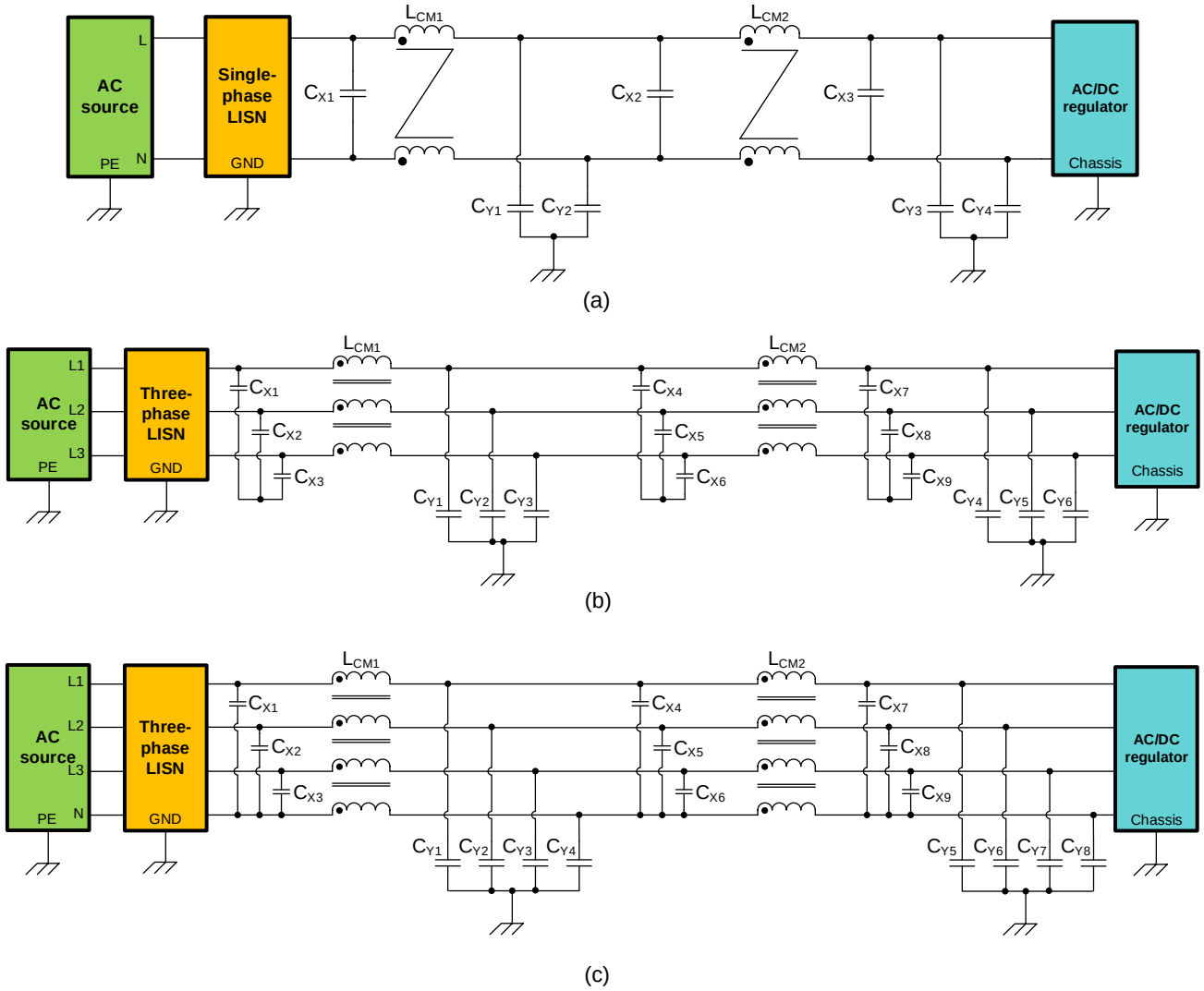

Fig. 3. Typical two-stage passive EMI filter for a single-phase system (a); a three-phase, three-wire system (b); and a three-phase, four-wire system (c).

Multistage filters as shown provide high rolloff and are common in high-power ac line applications where CM noise is typically much more challenging to mitigate than differential-mode (DM) noise. Although Fig. 3 omits components for input surge protection, overcurrent protection and X-capacitor resistive discharge, it does

include a line impedance stabilization network (LISN) in series with the input supply to enable measurement of total EMI, including DM and CM propagation components quantified separately using splitters.

At a higher level, passive EMI filters represent an intuitive, straightforward and traditional approach to mitigate the conducted emissions of a power electronics circuit, even though the size, weight and cost of the passive components cause significant constraints in some applications. Such passive filter designs rely on the insertion of high-impedance series elements (DM inductors, CM chokes) and low-impedance shunt elements (X- and Y-capacitors) to create an impedance mismatch in the EMI current propagation path. The low-order switching harmonics usually dictate the size of the reactive filter components based on the required corner frequency (or multiple corner frequencies in multistage designs).

Taking the single-phase schematic in Fig. 3a as an example, CM chokes L_{CM1} and L_{CM2} and Y-rated capacitors C_{Y1} to C_{Y4} (connected from the ac power lines to earth ground) provide CM attenuation. The CM current sourced from the switching regulator returns first through the regulator-side Y-capacitors and next through the Y-capacitors positioned between CM chokes. The alternative return path of any remaining CM current is through the measuring impedance of the LISN setup—obviously detrimental to EMI performance.

As mentioned in the introduction, safety regulations limit the total Y-capacitance to relatively low values (typically less than 30 nF), and the CM inductance of the chokes required for a desired corner frequency ($=1/\sqrt{LC}$) is relatively high, often in the range of 1 mH to 5 mH—making the chokes large, heavy and expensive. In contrast, X-capacitors C_{X1} to C_{X3} can be large-valued (typically 2.2 µF) and provide sufficient DM attenuation along with the leakage inductance of the CM chokes or a dedicated small-sized DM filter inductor.

In effect, CM chokes dominate the size of the EMI filter, as illustrated by the practical implementation[5] in Fig. 4, and reveal several challenges during EMI filter design—including bulky volume, thermal management issues, acoustic noise, filter resonances and electromagnetic coupling between components. In addition, parasitic elements of the filter components (especially CM chokes) affect high-frequency performance and achievable attenuation. The discrete components used in the filter come in different form factors from various manufacturers and are not optimized to fit well with one another, compromising the spatial design and assembly of the filter solution.

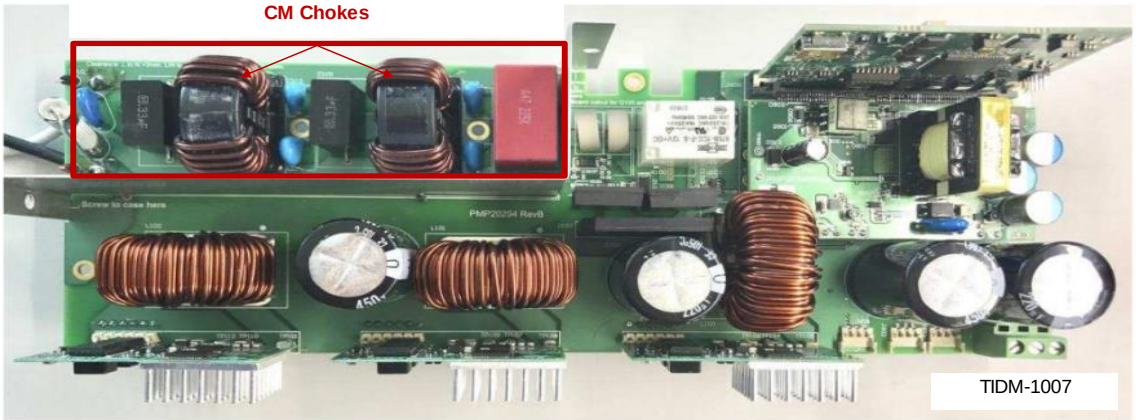

Fig. 4. Conventional single-phase passive EMI filter in a totem-pole PFC reference design.

The volume of the passive filter is clearly one of the limiting factors for increasing power density, especially as advances in passive components lag behind high-speed (wide-bandgap) power semiconductors and circuit topologies. Practical filter implementations can occupy as much as 30% of the total volume of a power solution. Where power density is an important metric, a smaller EMI filter is mandatory.

AEFs

There have been numerous publications[6-8] about the application of AEFs, with results yielding a substantial reduction in filter size and volume relative to a conventional passive-only solution. Much like a passive EMI filter, the AEF circuit connects to the lines between the EMI source and the EMI victim, as shown in Fig. 5. Unlike a passive filter, however, an AEF circuit uses active devices and control to sense the residual (DM or CM) voltage or current disturbance, and injects an opposing signal that directly negates that noise disturbance.

Based on the superposition theorem of signals with equal amplitude and opposite phase, the injected voltage or current should theoretically cancel or nullify the incident noise voltage or current contribution from the EMI source—essentially a destructive interference. This strategy is commonly applied in acoustics and successively for EMI.

The expectation is that an AEF significantly reduces EMI, resulting in a smaller-size filter versus a traditional passive-only design with equivalent attenuation. Along with an AEF, other (smaller) passive components can interface to the power stage and improve the overall attenuation—these circuits are known as hybrid EMI filters (HEFs).

The design and implementation of AEF and HEF circuits depend on the path of conduction (DM or CM) and the required sensing, gain and injection stages. As shown in Fig. 5, the cancellation signal is directly generated from a measured signal by feedback or feedforward approaches.

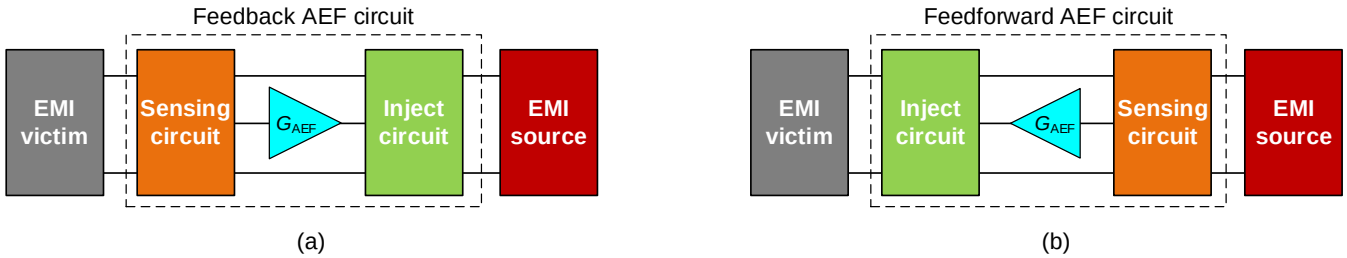

Fig. 5. The sensing, gain and injection stages of an AEF. The control structure could be feedback with high gain (a) or feedforward with unity gain (b).

A previous EMI article series in How2Power Today described several AEF techniques to diminish the reliance on bulky passive filter components, along with active-filter structures generalized according to the sensed noise parameter (voltage or current), the means by which the cancellation signal is injected (voltage or current), and the active control technique (feedback or feedforward).[3]

Defining The CM Active Filter Circuit

Since magnetic components for both current sensing and voltage injection are large-sized, and likely custom parts (offsetting the size reduction that an AEF enables), it's a good idea to select an AEF topology that precludes the use of additional magnetic components. The voltage-sense current-inject (VSCI) implementation leverages capacitors in combination with low-voltage active circuits for sensing and injection, and thus achieves a smaller size.[3]

Fig. 6 shows a simplified single-phase schematic to illustrate the basic principle of the selected feedback-VSCI circuit in a CM filter setup. As mentioned previously, the main idea with this AEF topology is to use an injection capacitor with a value similar to the Y-capacitance in an equivalent passive filter in order to reduce the values of the CM chokes, which are the largest components in high-power filters.

The Thévenin-equivalent CM noise source consists of voltage source v_S in series with source impedance Z_S, which is considered capacitive. The mains impedance Z_{GRID} is typically inductive. CM chokes, designated as L_{CM1} and L_{CM2}, also function as series decoupling elements to achieve high source and load impedances, as required for a high-attenuation feedback-VSCI design.

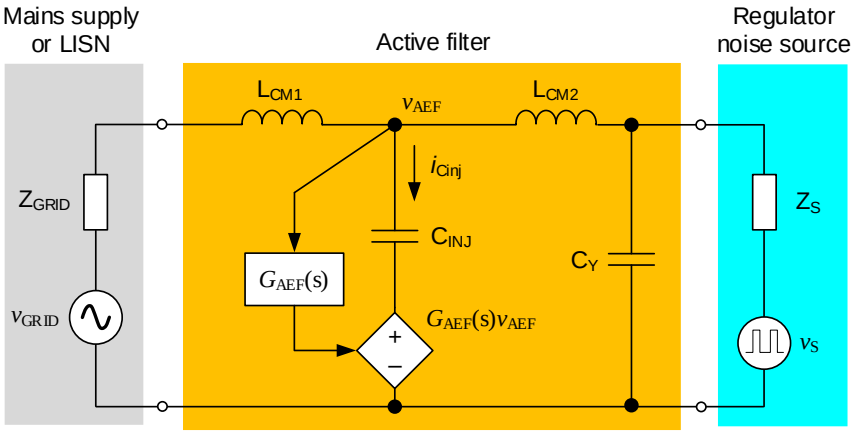

Fig. 6. Simplified schematic to illustrate basic principles for CM filtering and injection capacitor multiplication.

With Y-rated sense and injection capacitors connected to the ac lines, the purpose of the circuit is to reduce the total filter volume, yet maintain low values of the low-frequency earth leakage current using an active circuit that shapes the frequency response of the injection capacitor—effectively increasing its value for high frequencies. In turn, this amplified injection capacitance over the frequency range of interest is the key to lowering CM choke inductances relative to values of a passive filter with equivalent attenuation.

The circuit advantages are:

- A simple filter structure with a wide operating frequency range and high stability margins.
- A reduced CM choke size for lower volume, weight, power loss and cost, while also resulting in better high-frequency performance given lower choke self-parasitics and a higher self-resonant frequency (f_{SRF}).
- No additional magnetic components—only Y-rated sense and injection capacitors, with minimal impact to peak touch current (measured according to IEC 60990[2]).
- Enhanced safety using a low-voltage AEF IC referenced to chassis ground.
- A standalone analog IC implementation that provides flexibility in terms of placement near the filter components.
- Surge immunity to input line voltage transients to help meet IEC 61000-4-5 (with appropriate voltage clamping internal or external to the IC).

Y-Capacitor Multiplication

An AEF circuit for CM noise mitigation either amplifies the apparent inductance of a CM choke or the apparent capacitance of a Y-capacitor over the frequency range of interest. A VSCI AEF configured for CM attenuation uses a power amplifier stage as a capacitive multiplier of the injection capacitor, C_{INJ}. It is this higher value of active capacitance that supports lower values for the CM chokes in order to achieve a target attenuation.

Referring to Fig. 6, equation 1 shows that the injection capacitance is effectively multiplied by G_{AEF}, the CM voltage gain from the power lines to the amplifier output:

$$v_{C_{INJ}} = \left[1 - G_{AEF}(f)\right] v_{AEF}$$

$$i_{C_{INJ}} = C_{INJ} \frac{dv_{C_{INJ}}}{dt} = \left[1 - G_{AEF}(f)\right] C_{INJ} \frac{dv_{AEF}}{dt}$$

$$\Rightarrow C_{INJ,active}(f) = \left|1 - G_{AEF}(f)\right| C_{INJ} \qquad (1)$$

Fig. 7 shows a simulated plot of an injection network impedance when enabling and disabling a feedback-VSCI AEF circuit. The lower impedance above 2 kHz (and especially above 100 kHz) is caused by the capacitive amplification from the active circuit of a 4.7-nF injection capacitor and its associated damping network.

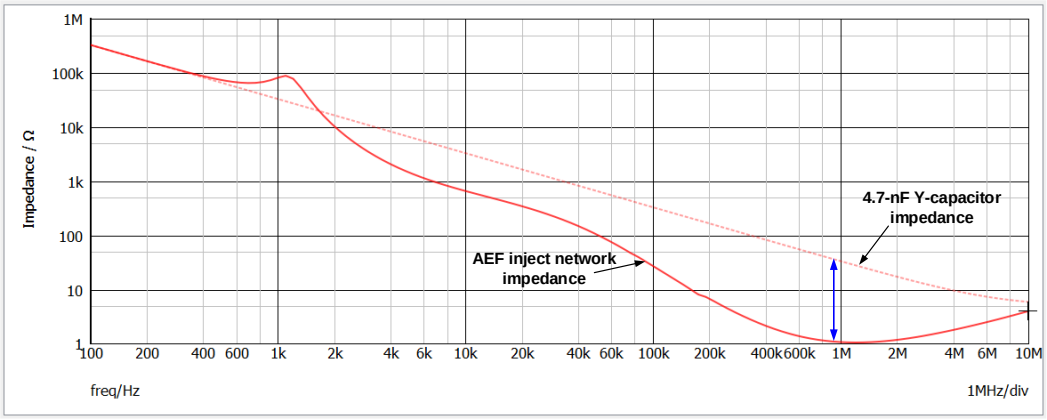

Fig. 7. Example of injection branch impedance Z_{INJ} with the AEF enabled vs. a conventional Y-capacitor, highlighting the increased equivalent capacitance obtained at higher frequencies through active feedback action.

Practical AEF Implementation

Fig. 8 shows practical AEF implementations for CM attenuation using the TPSF12C1 and TPSF12C3 standalone AEF ICs[9-11] in single-phase and three-phase power systems, respectively.

The setups are derived from the passive-only filters as shown by positioning the AEF IC and injection capacitor at the center node between the CM chokes to provide a lower-impedance shunt path for CM currents. The sense pins of this device family interface with the power lines using a set of Y-rated sense capacitors, typically 680 pF, and feed into a high-pass filter and signal combiner, as shown in the IC block diagram of Fig. 9. The IC rejects both the line-frequency (50- or 60-Hz) ac voltage as well as DM disturbances, while amplifying high-frequency CM disturbances and maintaining closed-loop stability using an external tunable damping circuit.

The components between the COMP1 and COMP2 pins form a lead-lag network that sets the amplification gain characteristic. The output of the amplifier at INJ injects the required noise-canceling signal back into the power lines through a damping and stability network (see the components with subscript "D" reference designators in Fig. 8), and a Y-rated injection capacitor C_{INJ}, typically 4.7 nF. The IC includes integrated filtering, compensation and protection circuitry. The VDD bias supply ranges from 8 V to 16 V, nominally 12 V, and references to the system chassis ground.

The X-capacitor(s) placed between the two CM chokes effectively provide a low-impedance path between the power lines from a CM standpoint, typically up to low-megahertz frequencies. This path allows current injection onto one power line (typically neutral, or the line routed nearest the IC) using only one injection capacitor. If the three-phase filter is a three-wire system without a neutral wire, the SENSE4 pin of the TPSF12C3 ties to ground and the injection capacitor connects to an artificial star-point connection of the X-capacitors.

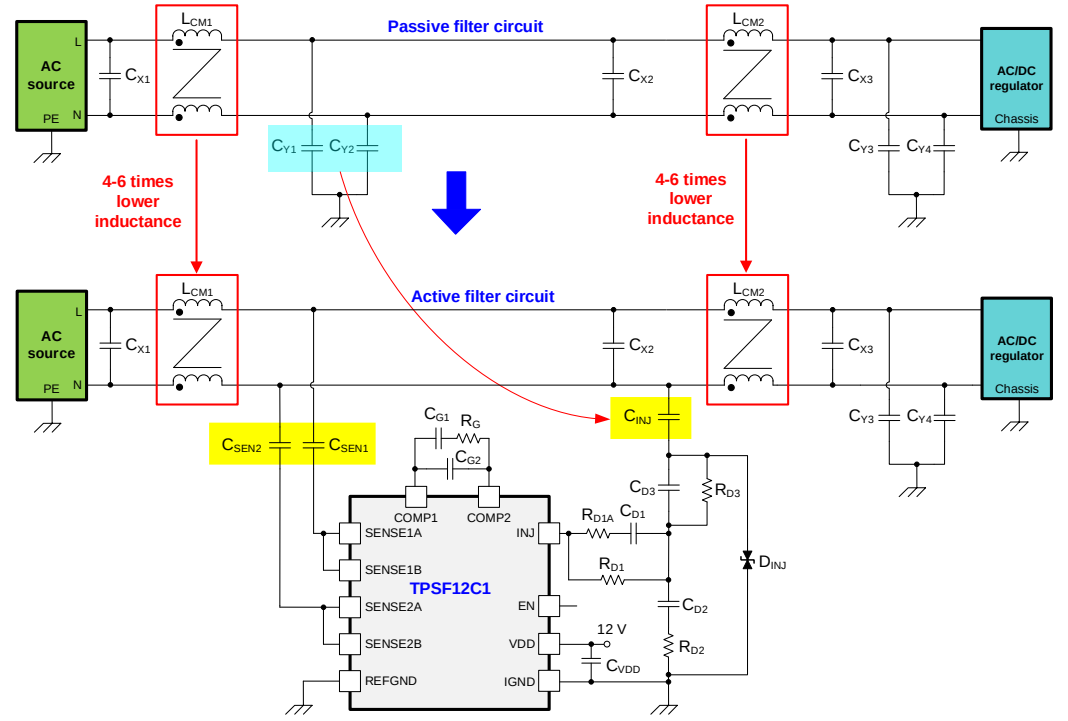

(a)

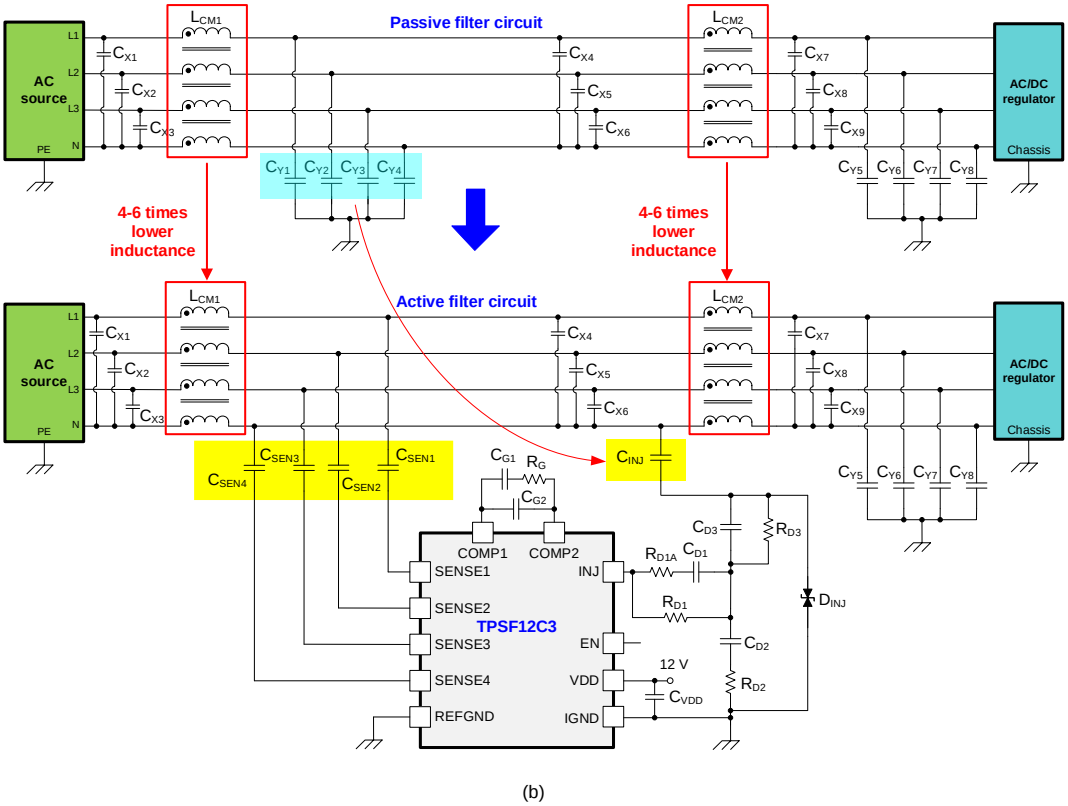

(b)

Fig. 8. AEF implementations for CM attenuation: a single-phase system (a) and a three-phase, four-wire system (b).

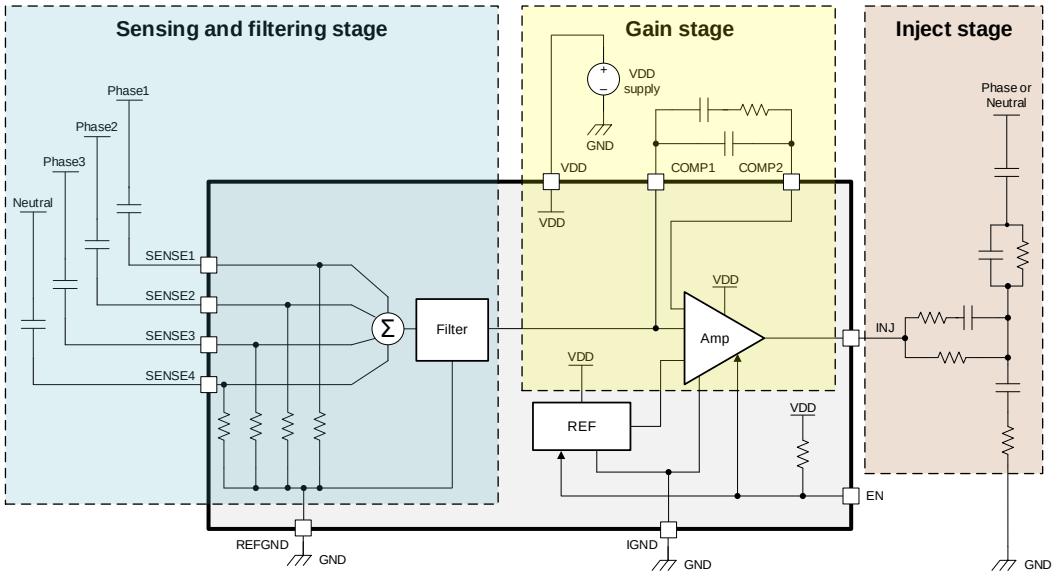

Fig. 9. Internal block diagram of the TPSF12C3 three-phase stand-alone AEF analog IC.

Experimental Results

Fig. 10 shows a practical AEF implementation using the TPSF12C1 single-phase AEF IC, suitable for the bridgeless PFC converter shown in Fig. 4.

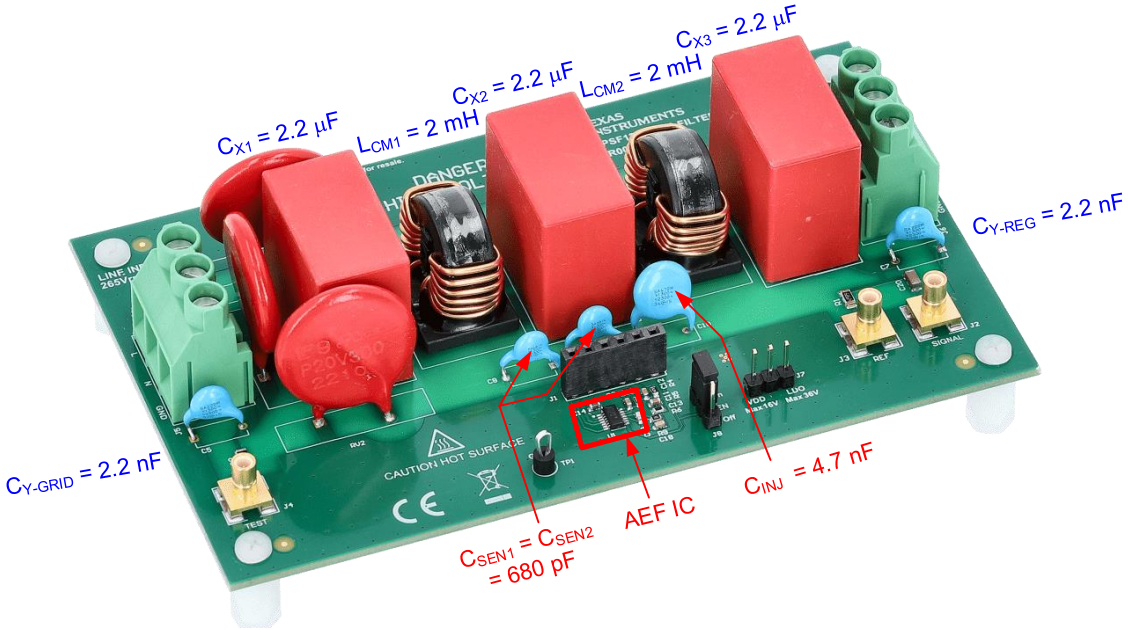

Fig. 10. Single-phase filter evaluation board with an AEF. The design is rated at 10 Arms.

Fig. 11 shows CM noise measurements with the AEF disabled and enabled.

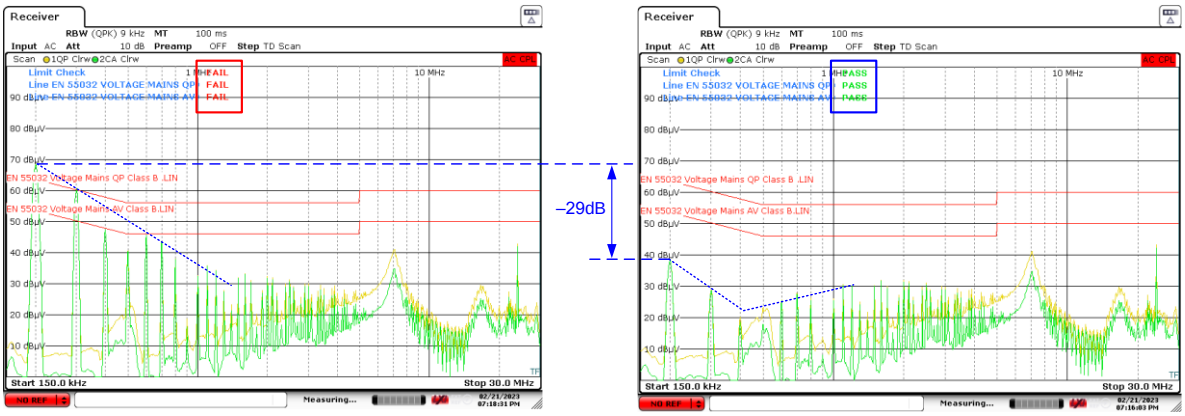

AEF disabled (a) AEF enabled (b)

Fig. 11. CISPR 32 Class B EMI results (CM noise only) with the AEF disabled (a) and enabled (b).

As evident in Fig. 11, the AEF design provides up to 30 dB of CM noise attenuation in the low-frequency range (100 kHz to 3 MHz), which enables a filter using two 2-mH nanocrystalline chokes to achieve CM attenuation performance equivalent to a passive filter design with two 12-mH chokes. To make a fair comparison, these chokes come from the same component family (made by Würth Elektronik) with a similar core material.

The table captures the applicable CM choke parameters for the passive and active designs, and Fig. 12 highlights the volume, footprint, weight and cost savings.

Table. CM choke parameters for the passive and active filter solutions.

Filter design	CM choke part number	Quantity	L_{CM1}, L_{CM2} (mH)	R_{DCR} (mΩ)	Size (L × W × H, mm)	Total mass (g)	Total power loss (W) at 10 A, 25°C
Passive	7448051012	2	12	15	23 × 34 × 33	72	6.0
Active	7448031002	2	2	6	17 × 23 × 25	20	2.4

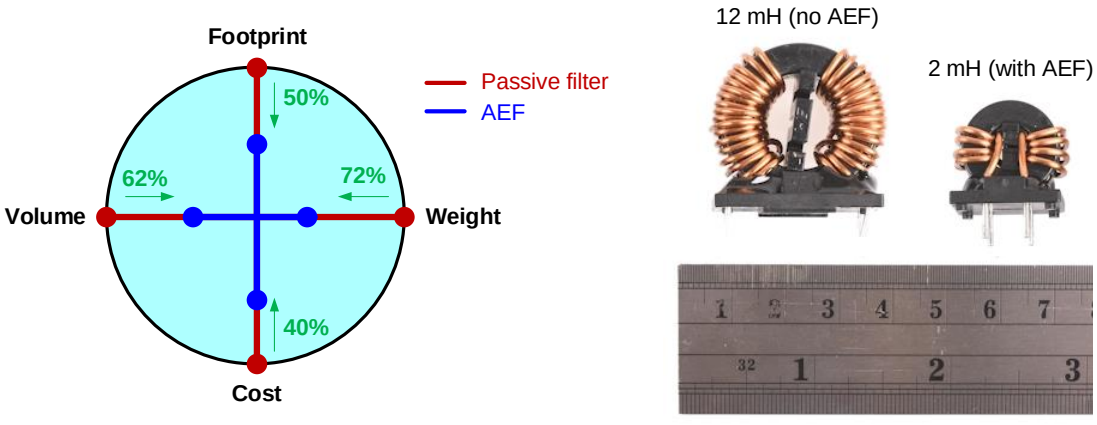

(a) (b)

Fig. 12. Footprint, volume, weight and cost reductions enabled by an AEF (a) and choke size comparison (b).

The AEF in this example achieves a 62% total copper loss reduction at 10 A (neglecting the winding resistance increase from the temperature rise), which implies lower component operating temperatures and improved reliability.

Fig. 13 provides impedance curves for the CM chokes to highlight the smaller-size CM choke, which has a higher self-resonant frequency and improved high-frequency performance. As an example of the higher CM impedance at high frequencies because of the lower intrawinding capacitance, the impedance of the choke at 30 MHz increases from 150 Ω to 2.2 kΩ (when going from 12 mH in the passive design to 2 mH in the active design). The × and o markers shown at 10 MHz and 30 MHz in Fig. 13 mark the impedances for passive and active designs, respectively. The higher choke impedance above 4 MHz for active designs largely obviates the need for high-frequency filtering with grid-side Y-capacitors.

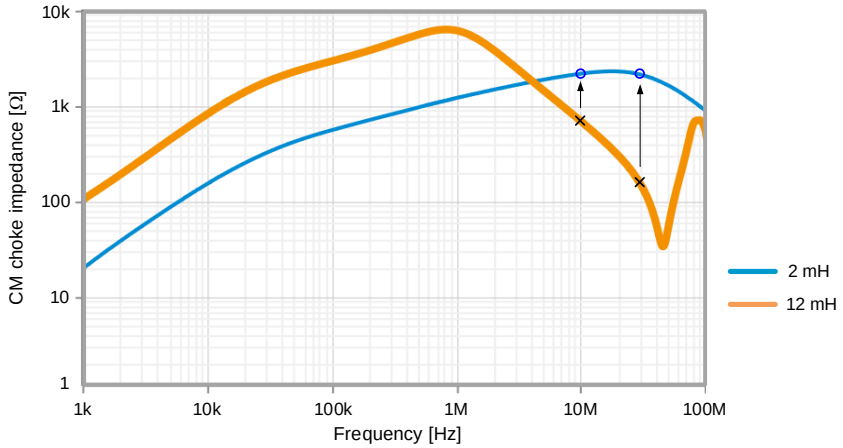

Fig. 13. Impedance characteristics of the selected CM chokes in the passive design (2 × 12 mH) and active design (2 × 2 mH).

As expected, horizontally mounted chokes in three-phase circuits can generally yield even larger percentage footprint reductions relative to the vertically mounted chokes common in single-phase designs. One caveat is that smaller-sized CM chokes have inherently lower leakage inductance, so DM noise may increase. Using a higher X-capacitance or adding a dedicated DM filter inductor can improve DM attenuation as needed.

Summary

A compact and efficient design for the EMI filter stage is one of the primary challenges in high-density switching regulator designs, particularly for automotive applications where solution size, weight and cost are important considerations. The shift of next-generation power electronics toward smaller packaging, higher densities, improved performance, reduced weight and lower cost necessitates a new approach to EMI filter design. To this end, the AEF circuit presented in this article is a viable means to enable significant improvements to the volumetric and gravimetric power density of the filter.

References

1. "Standard for Safety DC Charging Equipment for Electric Vehicles, 3rd Edition," Underwriters Laboratories (UL) 2202, Northbrook, Illinois, Dec. 15, 2022.
2. "Methods of Measurement of Touch Current and Protective Conductor Current," IEC 60990, Edition 3.0. IEC: Geneva, Switzerland, May 30, 2016.
3. "The Engineer's Guide To EMI In DC-DC Converters (Part 17): Active And Hybrid Filter Circuits" by Timothy Hegarty, How2Power Today, April 2021 issue.
4. "An Overview of Conducted EMI Specifications for Power Supplies" by Timothy Hegarty, TI white paper, literature No. SLYY136, February 2018.
5. "High Efficiency GaN CCM Totem Pole Bridgeless Power Factor Correction (PFC) Reference Design," Texas Instruments reference design No. TIDM-1007, accessed Sept. 25, 2023.

6. "A Survey of Active EMI Filters for Conducted EMI Noise Reduction in Power Electronic Converters" by Balaji Narayanasamy and Fang Luo, IEEE Transactions on Electromagnetic Compatibility 61, no. 6 (December 2019): pp. 2040-2049.
7. "An Active EMI Filter for Common-Mode EMI Mitigation in High-Power AC Systems" by Timothy Hegarty, Ashish Kumar, Robert Blattner, and Abdallah Obidat, PCIM Europe 2023 International Exhibition and Conference, May 9-11, 2023, pp. 1-6.
8. "How Active EMI Filter ICs Mitigate Common-Mode Emissions and Increase Power Density in Single- and Three-Phase Power Systems" by Timothy Hegarty, Texas Instruments white paper, literature no. SLVAFJ9, March 2023.
9. "Power-supply filter ICs" Texas Instruments, accessed Oct. 19, 2023.
10. TPSF12C1 common-mode active EMI filter (AEF) for single-phase systems, Texas Instruments, accessed Oct. 19, 2023.
11. TPSF12C3 common-mode active EMI filter (AEF) for three-phase systems, Texas Instruments, accessed Oct. 19, 2023.

About The Author

Timothy Hegarty is a senior member of technical staff (SMTS) in the Switching Regulators business unit at Texas Instruments. With over 25 years of power management engineering experience, he has written numerous conference papers, articles, seminars, white papers, application notes and blogs. Tim's current focus is on enabling technologies for high-frequency, low-EMI, isolated and nonisolated regulators with wide input voltage range, targeting industrial, communications and automotive applications in particular. He is a senior member of the IEEE and a member of the IEEE Power Electronics, Industrial Applications and EMC Societies.

For more on EMI and EMC topics in power supply design, see the How2Power's Power Supply EMI Anthology.